Hindawi
Mathematical Problems in Engineering
Volume 2019, Article ID 7860214, 12 pages
https://doi.org/10.1155/2019/7860214

Research Article

A Game Theory Energy Management Strategy for a Fuel Cell/Battery Hybrid Energy Storage System

Qiao Zhang and Gang Li

The School of Automobile and Traffic Engineering, Liaoning University of Technology, Jinzhou 121001, China

Correspondence should be addressed to Qiao Zhang; zq_625@163.com

Received 8 November 2018; Accepted 16 December 2018; Published 9 January 2019

Academic Editor: Denizar Cruz Martins

Copyright © 2019 Qiao Zhang and Gang Li. This is an open access article distributed under the Creative Commons Attribution License, which permits unrestricted use, distribution, and reproduction in any medium, provided the original work is properly cited.

This paper introduces a game theory approach to implement power flow distribution mission for a fuel cell/battery hybrid system considering uncertain power information. To fully describe the vying interaction relationship between the fuel cell and the battery, we design the power distribution problem as a noncooperative game problem, in which the fuel cell and the battery are deemed to be two interactional players, and each one chooses proper amount of power supply to maximize its own optimization function relying on the other chosen. Different from all previous research work in the published papers, the power demand information of the adopted driving cycle is assumed to be absolutely known. In this paper, we discuss the case that when the power demand is uncertain how the players act and the Nash Equilibrium can be effectively achieved. Three original contributions are made. First, we develop the utility function for each player taking into account the uncertain behavior of the power demand due to inaccurate prediction of driving cycle. Second, an iterative algorithm with a fuzzy logical controller for correction is proposed to reduce the influence of uncertain power demand information on the decisions of the players. Finally, the effectiveness is validated by a comparison simulation test.

1. Introduction

In the last two decades, the worsening environment and energy shortage problem have brought significant challenge to the global automotive industry. Again, new energy vehicles, which are powered using alternative energy for replacing traditional gasoline and diesel oil, have been paid more close attention [1–3]. Of all the candidate energy storage devices, the fuel cells are supposed to be good potential for directly superseding automobile internal combustion engines to power electric vehicles with considerable driving range for users. However, the slow dynamic response of the fuel cells will directly influence vehicle speed-up and speed-down performance. In addition, the fuel cells cannot supply negative power demand, which thus give a limit to recover the braking energy of the vehicle. To correct for these flaws and improve vehicle performance, the fuel cell hybrid systems have been suggested in the literature for practical vehicle application. In a fuel cell hybrid system, a battery or a supercapacitor pack is usually considered as auxiliary device for supply the drastic components of the power demand [4–6].

For a fuel cell/battery hybrid system, energy management control strategy is crucial for exploiting the advantages of the hybridization by coordinating the power flow between the fuel cell and the battery. State machine energy strategies were introduced to realize the state switch of the fuel cell and the battery to satisfy the load power demand as well as maintain the energy level within predefined range in [7, 8]. This strategy is simple and effortless for online implementation. However, the strategy lacks flexibility and adaptation to variation of the load power demand due to the limit of these fixed rules. To deal with complex and uncertain variable relation of the control strategy, fuzzy controllers were developed for a fuel cell hybrid system [9, 10]. Compared with the state machine strategy, the control performance can be improved to some extent due to improved flexibility and adaptation. However, the two types of strategies mentioned above are developed based on predefined deterministic or fuzzy logical rules, which largely depend on knowledge and

experience of a designer. Therefore, these strategies cannot achieve optimal control performance.

To obtain enhanced control performance, the rules of the strategies are often optimized using an offline optimization algorithm for a given driving cycle. The introduced algorithms include genetic algorithm [11], particle swarm optimization [12], simulated annealing optimization [13], DIRECT global optimization [14], and dynamic programming algorithm [15]. However, these optimization algorithms are centralized and only deal with single objective optimization problem. When a system has multiple optimization objectives, they are usually weighted and transformed into a single objective function to optimize using these algorithms. These weights were usually set to be fixed and rely on the preferences of the designers. In this way, however, the interaction between the competing optimization objectives (such as hydrogen economy and battery life cost) cannot be captured fully and the optimization result therefore lacks of objectivity.

Game theory provides one promising solution to the centered optimization dilemma by implementing independent optimization operation for each control object. Owing to its unique advantage in dealing with interaction and conflicting interests for coupled multiagent system, they have been widely applied to smart grid for demand response management [16–18] and sustainable energy system planning problem [19]. Some literatures have reported its successful application for energy management in different hybrid systems. A game theory (GT) controller was developed to capture tradeoff between driver operation and vehicle performance for a JLRF2 HEV in [20]. This application anticipates that the driving style of the driver is intrinsically coupled with vehicle fuel economy and emission performance. Test conclusions indicated that the GT control strategy by less calibration cost could achieve better performance compared with the baseline control for real world driving cycles. In [21], the GT strategy is applied for a fuel cell/battery/supercapacitor hybrid system to maximize a payoff function consisting of powertrain efficiency and vehicle performance. Simulation conclusions demonstrated the GT approach could benefit the two objectives simultaneously. Another example of the GT to energy management for an engine/battery/supercapacitor hybrid system is described in [22]. The author formulated a current control problem among the three power sources using noncooperative game theory approach. It was analytically proved that the Nash equilibrium can be iteratively calculated and the preference of each player, namely, the fuel consumption and battery life, could be satisfied simultaneously.

For energy management problem of hybrid system, each power source is personalized as a participant and which chooses certain amount of power supply to maximize its own optimization function depending on the actual power demand of driving cycle, which can be predictively obtained by employing some predictive algorithms, such as neural network [23], support vector machine [24], and Markov chain models [25], as well as advanced sensor technologies, such as radar [26] or geographic information system (GPS) [27]. For most of previous research works, the games are developed based on the assumption that the prediction is completely accurate. The decision of each participant is completely believable. From the opposite perspective, this paper focuses on the problem when the predictive driving cycle information is inaccurate and how the players in the game to adjust their individual strategies and achieve their final equilibrium. The main contributions that are fundamentally different from prior research in the literature are summarized as follows. First, we propose the game scenario that the players make their decisions encountering uncertain power demand information. Second, an iterative algorithm with a fuzzy logical controller for correction is proposed to ensure that the Nash Equilibrium can be effectively reached. Finally, the effectiveness is validated by a comparison simulation test.

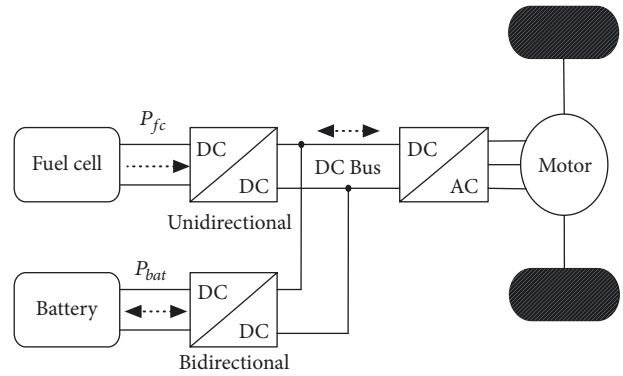

Figure 1: The fuel cell/battery hybrid topology adopted in this study.

The remainder of the paper is organized as follows. Section 2 presents the fuel cell and the battery hybrid energy storage system modeling. The game theory energy management strategy considering uncertain power information is described in Section 3. A case study is given to evaluate the effectiveness of the strategy in Section 4, followed by conclusive remarks in Section 5.

2. Hybrid Energy Storage System Modeling

The object plant of this study is a fuel cell/battery hybrid energy storage system with parallel topology structure, as shown in Figure 1.

2.1. Modeling of Fuel Cell. Owing to energy conversion loss, the actual yielded voltage of a fuel cell can be described by the following expression:

$$U_{cell} = E_{cell} - U_{act} - U_{ohmic} \tag{1}$$

where U_{cell} is actual yielded voltage, E_{cell} is Nernst voltage, U_{act} is awaken voltage, and U_{ohm} is internal resistance voltage. The Nernst voltage can be written by

$$E_{cell} = E_{cell}^{0} - k_E (T - 298) + \frac{R \cdot T}{2F} \ln \left[p_{H_2} \cdot \left(p_{O_2} \right)^{0.5} \right] - E_{delay} \tag{2}$$

where E_{cell}^{0} is fuel cell open-circuit voltage, k_E is experience factor, T is kinetic temperature, R is air coefficient, F is

Table 1: Parameters used in fuel cell model.

Parameters	Value
Voltage coefficient k_e [V/K]	0.000785
Kinetic temperature T [K]	358
Gas constant R [J/(kmol)]	7314.47
Faraday's constant F [C/kmol]	94484600
Molar coefficient of hydrogen k_{H_2} [kmol/atm s]	5.22 e-5
Course coefficient τ_{H_2} [s]	2.37
Molar coefficient of Oxygen k_{O_2} [kmol/atm s]	4.11 e-5
Fixed factor λ_e [Ω]	0.00452
Delay coefficient τ_e [s]	90
Flow size γ_{H-O}	1.0779
Use efficiency U	0.75
Voltage coefficient α_1	-0.8714
Voltage coefficient α_2	0.00214
Voltage coefficient α_3	8.01e-5
Voltage coefficient α_4	-1.65e-4
Internal resistance R_{ohm} [Ω]	0.002

Faraday constant, p_{H_2} is hydrogen flow stress, p_{O_2} is oxygen flow stress, and E_{delay} is reaction delay effect. p_{H_2}, p_{O_2} and E_{delay} can be calculated by the following variable relations:

$$p_{H_2}(s) = \frac{1}{k_{H_2}\left(\tau_{H_2} \cdot s + 1\right)}\left(q_{H_2}^{in} - 2k_r I\right) \tag{3}$$

$$p_{O_2}(s) = \frac{1}{k_{O_2}\left(\tau_{O_2} \cdot s + 1\right)}\left(q_{O_2}^{in} - k_r I\right) \tag{4}$$

$$E_{delay}(s) = \lambda_e I(s)\frac{\tau_e \cdot s}{\tau_e \cdot s + 1} \tag{5}$$

where k_{H_2} is molar coefficient of hydrogen reaction, τ_{H_2} is course coefficient of hydrogen reaction, $q_{H_2}^{in}$ is flow of hydrogen input-output, k_r is correction factor, k_{O_2} is molar coefficient of oxygen reaction, τ_{O_2} is course coefficient of oxygen reaction, $q_{O_2}^{in}$ is flow of oxygen input-output, λ_e is fixed factor, and τ_e is delay coefficient of input-output flow. The hydrogen and oxygen flow rate of fuel cell can be depicted as follows:

$$q_{H_2}^{in} = \frac{N \cdot I}{2F \cdot U} \tag{6}$$

$$q_{O_2}^{in} = \frac{1}{\gamma_{H-O}} q_{H_2}^{in} = \frac{N \cdot I}{2\gamma_{H-O} F \cdot U} \tag{7}$$

where γ_{H-O} is flow size and U is use efficiency.

The awaken voltage U_{act} is written as function of current and temperature as follows:

$$U_{act} = \alpha_1 + \alpha_2 \cdot T + \alpha_2 \cdot T \cdot \ln\left(I_{FC}\right) + \alpha_4 \ln\left(C_{O_2}\right) \tag{8}$$

where α_i, i=1,2,3,4, is a constant coefficient and C_{O_2} is oxygen AOEL, which is given by

$$C_{O_2} = \frac{P_{O_2}}{5.08 \times 10^6 \exp\left(-498/T\right)} \tag{9}$$

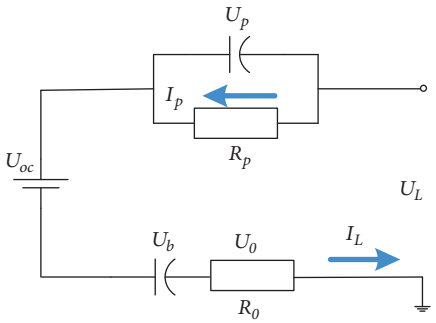

Figure 2: The equivalent circuit model for modeling the battery.

The internal resistance voltage U_{ohm} is direct proportion to current when the resistance is assumed to be a constant.

$$U_{ohmic} = I_{FC} \cdot R_{ohm} \tag{10}$$

Finally, the total voltage of the fuel cell stack with N cells in series can be calculated by

$$E_{FC} = N \cdot E_{cell} \tag{11}$$

The specific parameters and their values used in the model are given in Table 1.

2.2. Modeling of Battery. The adopted battery equivalent circuit model in this study is illustrated in Figure 2.

According to the electrotechnics principle, the work voltage of the battery is induced by

$$U_L = \begin{bmatrix} -1 & -1 \end{bmatrix} \cdot \begin{bmatrix} U_b \\ U_p \end{bmatrix} - R_0 \cdot I_L + U_{oc} \tag{12}$$

where U_L is the work voltage of the battery, I_L is the work current of the battery, U_p is capacitance terminal voltage, and

Table 2: Battery parameters and specific values.

Parameters	Value
Battery Type	Lithium-ion battery
Nominal pack voltage [V]	280
Nominal pack capacity [Ah]	40
Number of cells	144
Parallel number	2
Normal cell voltage [V]	3.9
Normal cell capacity [Ah]	20

R_0 is the internal resistance. The work current can be obtained by the following equation:

$$I_L = \frac{U_T - \sqrt{(U_T)^{1/2} - 4R_0P_L}}{2R_0} \tag{13}$$

where P_L is load power demand.

In the circuit, the voltage U_p and current I_p are used to describe Polarization effect of the small RC branch and can be obtained by

$$U_p = R_p \cdot I_p \tag{14}$$

$$I_{p,k} = 1 - \frac{\theta}{T} + \exp(-T) \cdot I_{p,k-1} + \left\{\frac{\theta}{T} - \exp(-T)\right\} \cdot I_{L,k-1} \tag{15}$$

where θ is related to time constant T and equal to $-\exp(-T) + 1$ $T = \Delta t/\tau$, and $\tau = RC$, and Δt is simulation step length.

The state of charge (SOC) of the battery is estimated by an ampere-hour integration method.

$$SOC = SOC_0 - k_{ch}k_{dis} \cdot \frac{\int \varphi \cdot I_{bat}dt}{C_{bat}} \tag{16}$$

In (16), the actual SOC is influenced by its initial energy state SOC_0, as well as battery coulomb efficiency φ and charging/discharging coefficients k_{ch} and k_{dis}. C_{bat} is nominal capacity supplied by manufacturer. The correlation parameter in the battery model is given in Table 2.

2.3. Modeling of DC/DC Converter. The DC/DC converter is used to control voltage of the fuel cell and the battery for satisfying different load power demand. Owing to frequent boost and buck operations, the efficiency of energy management is largely influenced by the DC converter. The efficiency curve of the adopted DC converter in this study is illustrated in Figure 3. It can be seen that the DC efficiency is related to voltage and current of the power source. Therefore the output power of the DC converter can be written by

$$P_{fc} = \frac{1}{\eta(I_{DC}, U_{DC})} P_{DC,fc} \tag{17}$$

$$P_{bat} = \frac{1}{\eta(I_{DC}, U_{DC})} P_{DC,bat} \tag{18}$$

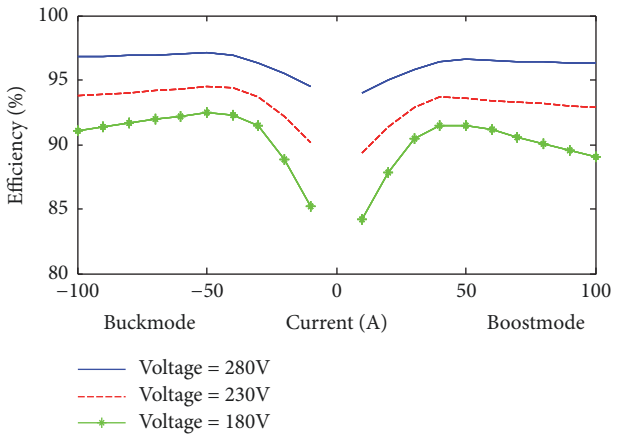

Figure 3: DC converter efficiency curve.

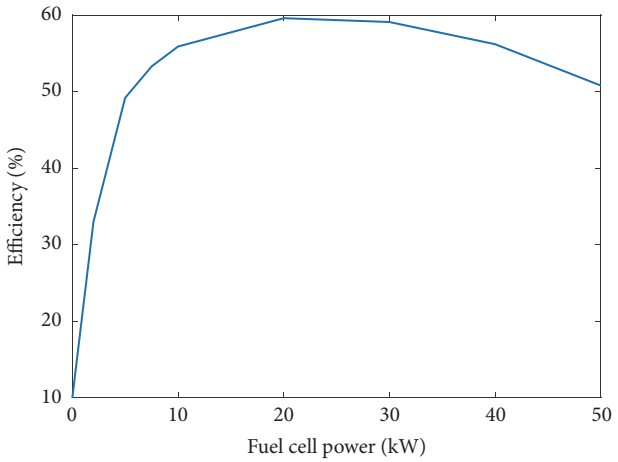

Figure 4: The fuel cell efficiency curve.

3. Game Theory Energy Management Strategy considering Uncertain Power Information

In this section, the optimization functions of the fuel cell and the battery are first developed. Based on the optimization functions, the optimal power values of each power source can be obtained. After that, we employ game theory formulation to describe the competing interaction between the fuel cell and the battery. In this study, the optimization objective of the fuel cell is to maximize its hydrogen economy.

The efficiency curve of a fuel cell with maximum 50 kW power capacity is shown in Figure 4. The efficiency data is obtained from ADVISOR software. It can be found that the hydrogen efficiency is directly related to fuel cell power. To assess the hydrogen consumption, the relationship between the hydrogen power and the net power needs to be first established. For this, a quadratic function is adopted and expressed by

$$P_h = a_1 \cdot P_{fc}^2 + a_2 \cdot P_{fc} + a_3 \tag{19}$$

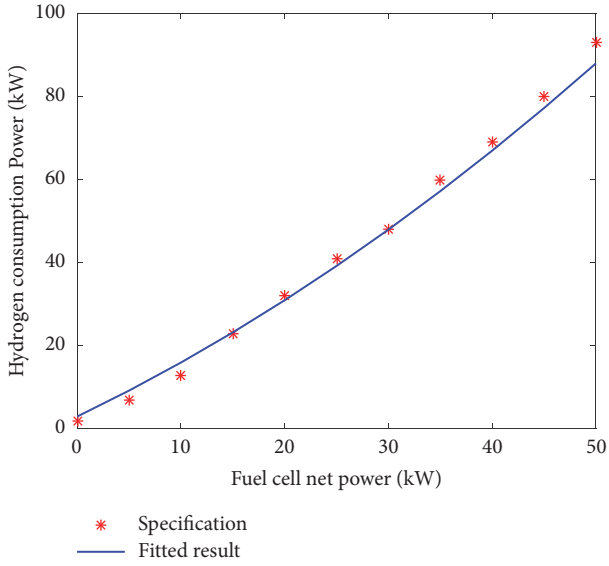

Figure 5: The fitted result of the hydrogen consumption.

where P_h is the hydrogen power of the fuel cell, P_{fc} is the net power of the fuel cell, and a_1, a_2, and a_3 are the fit coefficients. The fitted result is shown in Figure 5.

Then, the objective function of the fuel cell can be formulated as follows:

$$Cost_{fc,h} = \frac{c_h}{L_h} \sum_{k=1}^{n} P_h(k) \tag{20}$$

where c_h is the unit hydrogen price (\$/g), c_h=0.00341\$/g [28], and L_h is the lower heating value of hydrogen (J/g).

For the battery, due to vulnerable nature to use conditions, its degradation is often considered as an optimization objective in energy management. In this study, a battery capacity model is adopted to quantify the battery degradation according to the charging/discharging conditions [29]. The degradation model is empirically built using the following mathematic description:

$$Q_{loss} = B \cdot e^{-((E_a + A \cdot C_{rate})/(R \cdot T_{bat}))} (A_h)^z \tag{21}$$

where B is the index coefficient, Q_{loss} is the actual capacity decrement of the battery, T is the Kelvin scale (K), E_a is the awaken energy (J mol^{-1}), and R is the air factor (J (mol^{-1}/k)$^{-1}$). z is the law coefficient of the battery power, C_{rate} is the charging/discharging rate, and A is the correct coefficient of *the* battery charging/discharging rate. All parameters used in the model are given in Table 3.

The actual charging/discharging amount of the battery is quantified by

$$A_h = \frac{1}{3600} \sum_{k=1}^{N} \left| \frac{P_{bat}}{U_{bat}} \right| \tag{22}$$

Table 3: Parameters of battery degradation model.

Item	Value
B	30330
E_a	31700
R	8.314
A	370.3
z	0.55

Considering the battery capacity degradation range from its nominal scale C_{bat} to 0.8 C_{bat}, therefore the cost function of battery degradation can be formulated as follows:

$$Cost_{bat\_degr}(k) = \frac{C_{bat} \cdot U_{bat} \cdot p \cdot A_h}{1000 \cdot 0.2} \times \exp - \left(\frac{31700 - 370.3 C_{rate}}{8.314 T_{bat}} \right) \tag{23}$$

where Q_{bat} is the normal capacity of the battery, U_{bat} is the normal voltage of the battery, and p is the capacity cost of the battery, p=1600\$/kWh [30].

For the descried topology structure in this study, the demands of the fuel cell are strongly coupled with that of the battery and their optimization objectives are competing; e.g., the hydrogen consumption cost can be reduced at the cost of sacrificing the battery degradation cost, and vice versa. For such a coupled hybrid system, it is crucially important to capture the tradeoff between the fuel cell and the battery. To achieve this purpose, we employ noncooperative game theory to formulate the competing interaction, in which one player strategically chooses the amount of the load power it could supply so as to maximize its own optimization function according to the load power demand and the strategy the other player adopted. In such a way, the two players can interact with each other and finally reach their equilibriums.

To clarify this problem, each component of the game formulation defined in the form $\Gamma = \{\{F, B\}, \{P_{fc}, P_{bat}\}, \{U_{fc}, U_{bat}\}\}$ will be explained fully as follows.

(1) Here, "F" represents the fuel cell, and "B" represents the battery. In the game, they act as two competing players and respond to each other.

(2) The strategy of each player is the power it could supply which corresponds to the amount of the power demand from the powertrain satisfying their individual constraints, such as current and power constraints.

(3) The utility function is used to quantify the level of satisfaction that the optimization objective of each player is achieved.

The utility function of each player is formed in quadratic form, which is continuous and quasiconcave in the strategy space for ensuring the existence of the Nash equilibrium and as well as its uniqueness. For the fuel cell, we consider the following utility function:

$$U_{fc} = c_{fc} - \alpha \left(P_{fc} - P_{fc,opt} \right)^2 - (1 - \alpha) \left[P_{fc} - \left(P_{load} - P_{bat,opt} \right) \right]^2 \tag{24}$$

In (24), c_{fc} is a constant coefficient and α is the weighting coefficient ($0 < \alpha < 1$). The item $(P_{fc} - P_{fc,opt})^2$ is used to quantify the closeness of the actual power and its optimal value that minimizes the hydrogen consumption cost. The item $[P_{fc} - (P_{load} - P_{bat,opt})]^2$ is used to quantify difference between the actual power supplied by the fuel and the load power demand based on the assumption that the battery minimum degradation cost is achieved.

The utility function in the same form is also applied for the battery and written by

$$U_{bat} = c_{bat} - (1-\alpha)\left(P_{bat} - P_{bat,opt}\right)^2 - \alpha\left[P_{bat} - \left(P_{load} - P_{fc,opt}\right)\right]^2 \tag{25}$$

The differential expressions of the utility function in (24) and (25) with P_{fc} and P_{bat} are derived as follows:

$$\frac{\partial U_{fc}}{\partial P_{fc}} = -2\alpha\left(P_{fc} - P_{fc,opt}\right) - 2(1-\alpha)\left[P_{fc} - \left(P_{load} - P_{bat,opt}\right)\right] \tag{26}$$

$$\frac{\partial U_{bat}}{\partial P_{bat}} = -2(1-\alpha)\left(P_{bat} - P_{bat,opt}\right) - 2\alpha\left[P_{bat} - \left(P_{load} - P_{fc,opt}\right)\right] \tag{27}$$

When the players try to pursue their individual minimum cost, mathematically we have

$$\frac{\partial U_{fc}}{\partial P_{fc}} = 0 \tag{28}$$

$$\frac{\partial U_{bat}}{\partial P_{bat}} = 0 \tag{29}$$

By solving the above two equations, the strategies for the fuel cell and the battery are explicitly described by

$$P_{fc} = \alpha P_{fc,opt} + (1-\alpha)\left(P_{load} - P_{bat,opt}\right) \tag{30}$$

$$P_{bat} = \alpha P_{bat,opt} + (1-\alpha)\left(P_{load} - P_{fc,opt}\right) \tag{31}$$

From (30) and (31), the Nash Equilibrium is the power sequence ($P_{fc,i}$, $P_{bat,j}$, i, j=1,2,. . .,N) that minimizes the hydrogen consumption and the battery degradation simultaneously. To reach the Nash Equilibrium, an iterative algorithm is needed to find the appropriate power pair at each instant by adjusting the weighting coefficient α. The specific iteration process is shown in Figure 6.

From Figure 6, the optimal powers $P_{fc,opt}$ and $P_{bat,opt}$ that, respectively, minimize hydrogen consumption and battery degradation costs are calculated using particle swarm optimization for a given driving cycle. Detailed description of the algorithm process is expounded in [31]. In this study, we assume that the given driving cycle is deviating from its real condition due to inaccurate prediction. In this case, the

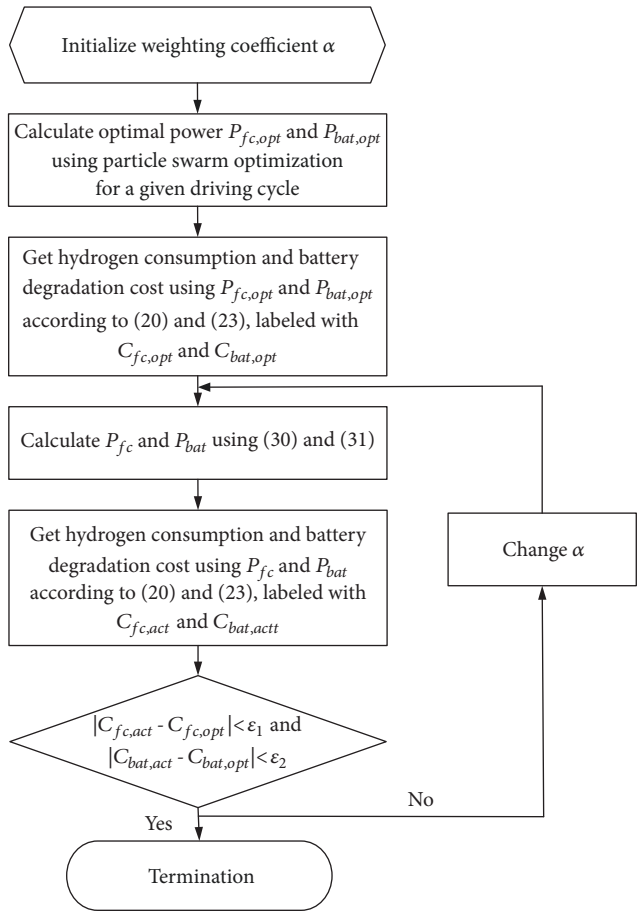

Figure 6: Flowchart of solving Nash equilibrium.

reliability of the optimal power $P_{fc,opt}$ and $P_{bat,opt}$ depends on prediction accuracy of driving cycle. To account for the influence of inaccurate information on the decisions of the players, the optimal powers $P_{fc,opt}$ and $P_{bat,opt}$ in the utility functions are weighted using a confidence coefficient. Then the utility function in (24) and (25) should be modified by

$$U_{fc} = c_{fc} - \left(1 - f\left(P_{fc,opt}\right)\right)\alpha\left(P_{fc} - P_{fc,opt}\right)^2 + \left(1 - f\left(P_{bat,opt}\right)\right)(1-\alpha) \cdot \left[P_{fc} - \left(P_{load} - P_{bat,opt}\right)\right]^2 \tag{32}$$

$$U_{\text{bat}} = c_{bat} - \left(1 - f\left(P_{bat,opt}\right)\right)(1-\alpha)\left(P_{bat} - P_{bat,opt}\right)^2 + \left(1 - f\left(P_{fc,opt}\right)\right)\alpha\left[P_{bat} - (P_{load} -) P_{fc,opt}\right] \tag{33}$$

where $f(\bullet)$ represents the confidence coefficient. The more accurate the prediction is, the smaller the coefficients are. In general, the prediction accuracy of the driving cycle can be evaluated using mean value (MV) and the standard deviation (SD) of prediction error for a given length prediction horizon. To analyze this problem, a fuzzy logic controller, as shown in Figure 7, is designed. The input variables of the fuzzy logic controller are the MV and the SD of prediction error and the

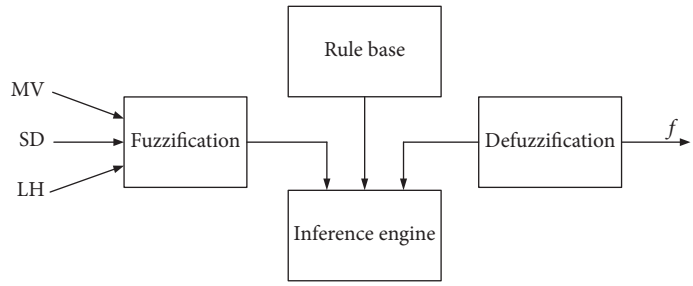

Figure 7: Structure of the fuzzy logic controller.

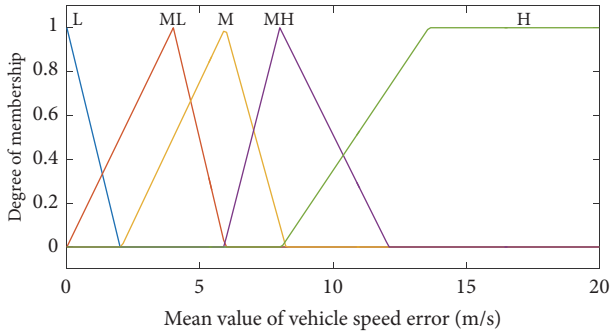

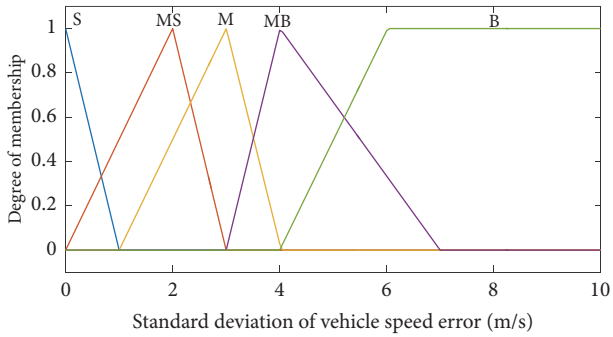

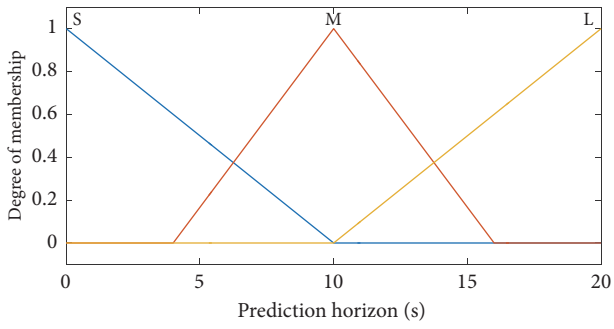

Figure 8: The membership functions of the input variables.

length of prediction horizon (LH); the output variable is the coefficient f.

In the fuzzy controller, the fuzzified descriptions of the input and output variables are realized by using the triangular membership function, which are shown in Figures 8 and 9. In the membership function, the MV and SD of the vehicle speed error are divided into five fuzzy subsets. Specifically,

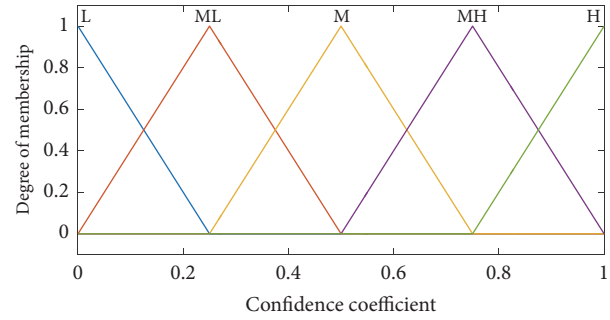

Figure 9: The membership functions of the output variable.

the MV includes "L (Low)", "ML (Medium Low)", "M (Medium)", "MH (Medium High)", and "H (High)". The SD includes "S (Small)", "MS (Medium Small)", "M (Medium)", "MB (Medium Big)", and "B (Big)". The LH is divided into "S (Short)", "M (Medium)", and "L (Long)". The confidence coefficient is divided into "L (Low)", "ML (Medium Low)", "M (Medium)", "MH (Medium High)", and "H (High)".

The MV and the SD are considered for each prediction horizon. Consequently, three subrule bases can be obtained and shown in Table 4.

4. Case Study

In this simulation study, the UDDS (Urban Dynamometer Driving Schedule) is adopted to serve as the actual driving cycle. An inaccurate prediction case is incorporated in the driving cycle, which is shown in Figure 10. The simulation vehicle main parameters are given in Table 5.

The prediction horizons are set to three different lengths, e.g., 5s, 10s, and 15s. When vehicle is running, for each prediction horizon, the mean value and standard deviation of the vehicle speed error can be online calculated according to the actual speed profile and the predictive result. The information is subsequently used by the fuzzy logic controller to calculate the confidence coefficient. For the purpose of performance comparison, the same two game theory based strategies are implemented with and without taking prediction error into consideration.

Figures 11–13 show the comparison results of the fuel cell power, the battery power, and SOC. In Figure 11, the prediction horizon is set to 5s. From Figure 11(a), it can be

Table 4: Three subrule bases.

(a) Rule base under short prediction horizon

MV/SD	S	MS	M	MB	M
L	H	H	MH	MH	M
ML	H	MH	MH	M	M
M	MH	MH	M	M	ML
MH	M	ML	ML	L	L
H	ML	L	L	L	L

(b) Rule base under medium prediction horizon

MV/SD	S	MS	M	MB	M
L	H	MH	MH	MH	M
ML	MH	MH	M	M	M
M	MH	M	M	ML	ML
MH	ML	ML	L	L	L
H	L	L	L	L	L

(c) Rule base under long prediction horizon

MV/SD	S	MS	M	MB	M
L	MH	MH	M	M	M
ML	M	M	M	ML	ML
M	ML	ML	ML	L	L
MH	L	L	L	L	L
H	L	L	L	L	L

Table 5: Vehicle main parameters.

Parameters	Amount	Unit
Mass	1550	kg
Frontal area	2.13	m^2
Tire radius	0.3	m
Drag coefficient	0.36	–
Rolling resistance coefficient	0.02	–

observed that the fuel cell power with prediction error into consideration is much smaller than that without prediction error into consideration. This is because the optimal power in the power distribution game, which has obvious effect on Nash equilibrium, e.g., the amount of the power distributed to each power source, is directly out of its real value due to the inaccurate prediction information. Consequently, the hydrogen consumption cost increases. This phenomenon becomes sometimes good or bad according to the actual prediction accuracy. When the fuel cell power increases, on the contrary, the battery power will be reduced while the power demand is supplied by the fuel cell and the battery together. Accordingly, the battery powers are compared and shown in Figure 11(b). Owing to less accumulated charging and discharging power in the case that the prediction error is ignored, hence the battery degradation cost is reduced. The cost is specifically listed in the Table 6. For 5s prediction horizon, the hydrogen consumption and battery degradation cost are 0.02068$ per kilometer and 0.009692$ per kilometer; hence the total cost is 0.03037$ per kilometer, which is smaller than that in the case that the prediction error is out of

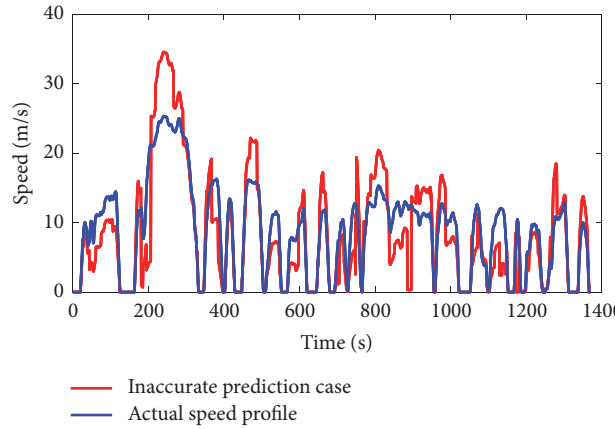

Figure 10: UDDS driving cycle and an inaccurate prediction case.

consideration. This is because the hydrogen consumption cost is obviously higher than the battery degradation cost. Although the total cost can be reduced by improving the battery power, the range is limited to the battery parameters, such as maximum power and state of charge.

Figures 12 and 13 show the power comparison of the fuel cell and the battery with 10s and 15s prediction horizon, respectively. It can be further found that the fuel cell power is improved as the prediction horizon is extended. Accordingly, the battery power is reduced and the total cost is increased. This phenomenon can be explained that when the prediction horizon is extended, more prediction errors get involved in predictive information, which leads to a relatively low reliability of the optimal power.

It can be further observed from the evolution of the battery SOC that a big SOC drop occurs at the time interval from 200s to 300s, in which the peak discharge power is effectively supplied by the battery. Two advantages can be found by the proposed consideration compared with the conventional one. First, the battery is reasonably controlled to supply peak power with less adverse influence of prediction error. Second, the battery SOC is always maintained within appropriate range. As a result, the battery always has enough space for absorbing the regenerative braking energy while satisfying the acceleration demand.

To further verify the effectiveness of the proposed strategy, a fuzzy logic controller is developed for a performance comparison. The controller has two inputs that are the load power and the battery SOC, and one output is the fuel cell power, which is illustrated in Figure 14.

In the developed fuzzy logical controller, the triangular membership functions are used for depicting the fuzzy relationships of load power, battery SOC, and fuel cell power within their possible variation range Figures 15–17. The load power has five membership functions including negative big (NB), negative small (NS), medium (M), positive small (PS), and positive big (PB). The negative power represents the power demand being absorbed by the hybrid system, and the positive power represents the power demand being supplied by the hybrid system. The battery SOC has three membership functions including low (L), medium (M), and high (H). In

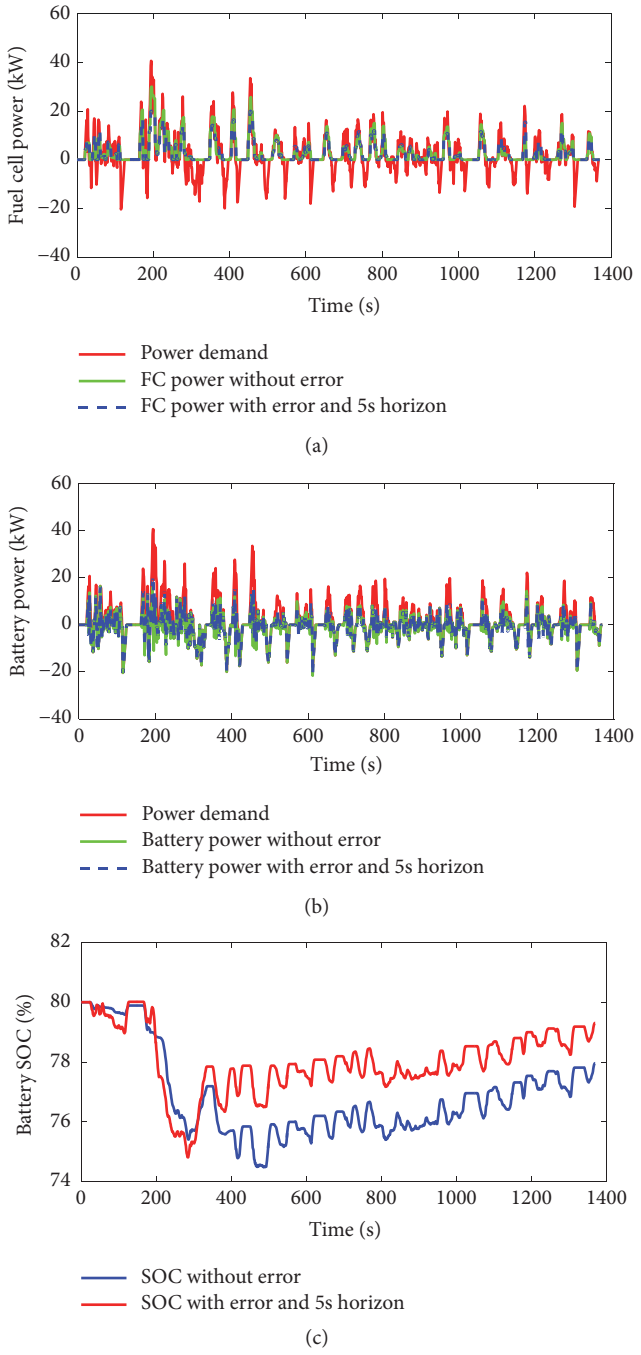

Figure 11: The power supplied by the fuel cell is compared in (a) and by the battery is in (b); the battery SOC is illustrated in (c). Note that here the prediction horizon is set to 5s.

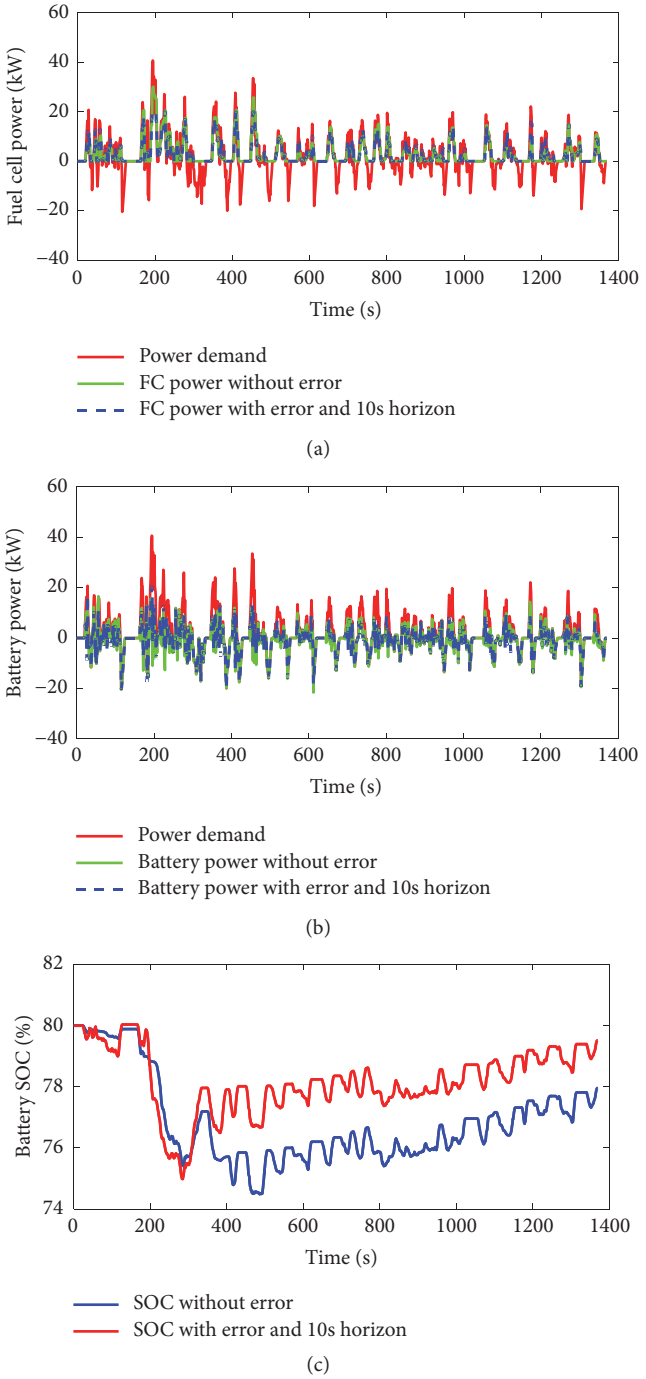

Figure 12: The power supplied by the fuel cell is compared in (a) and by the battery is in (b); the battery SOC is illustrated in (c). Note that here the prediction horizon is set to 10s.

this controller, the reference battery SOC is assumed to be 0.8. If the battery SOC is low, more regenerative power should be distributed to the battery; on the contrary, if the battery SOC is high, the minimum power should be withdrawn from the fuel cell regardless of the load power. The case where battery SOC is medium, the fuel cell power should be controlled to adapt to variation of the load power. The fuel cell power has four membership functions including small (S), medium (M), big (B), and too big (TB). The fuzzy logic rule base is given in Table 7.

Two strategies are both implemented on the condition that the driving cycle prediction is inaccurate, as shown in Figure 10. The simulation results are given in Figures 16–18. From Figure 16, it can be observed that the peak power and regenerative power of the load can be more effectively

Table 6: Comparison of hybridrogen consumption and battery degradation cost.

	hydrogen ($/km)	Degradation ($/km)	Sum cost($/km)
5s horizon	0.02068	0.009692	0.03037
10s horizon	0.02169	0.008825	0.03052
15s horizon	0.02123	0.009292	0.03052
Without error	0.02486	0.007533	0.03239

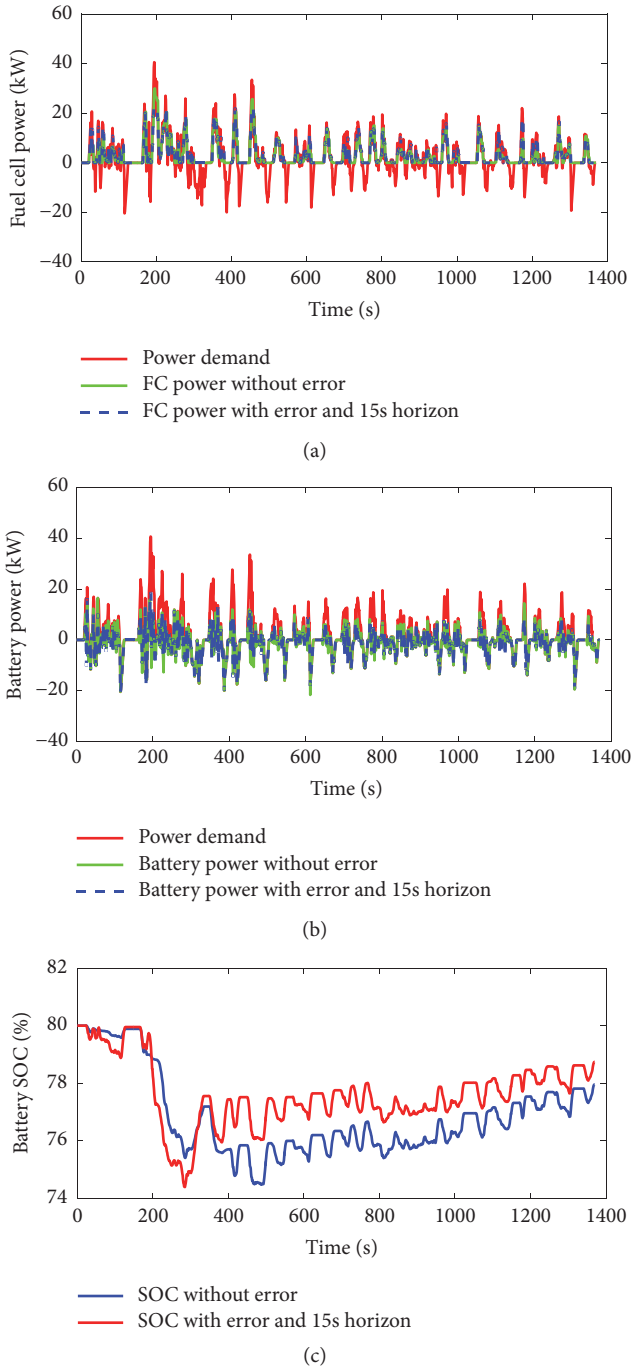

Figure 13: The power supplied by the fuel cell is compared in (a) and by the battery is in (b); the battery SOC is illustrated in (c). Note that here the prediction horizon is set to 15s.

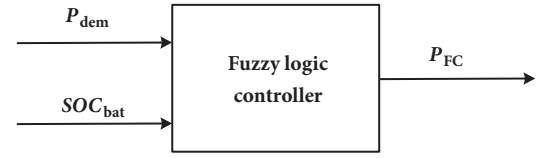

Figure 14: Fuzzy logic controller and its inputs and output.

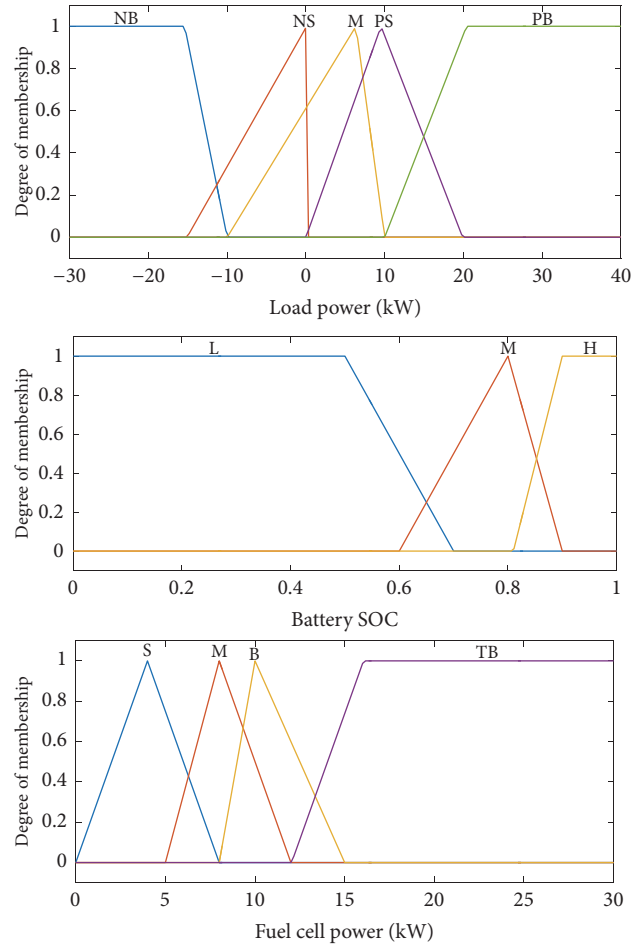

Figure 15: Membership functions of battery power, battery SOC, and fuel cell power.

absorbed by the battery using the proposed strategy compared with the fuzzy logic. Benefitting from this, the fuel battery power is shaved and smoothed (clearly seen from Figure 17), which could potentially extend the life of the fuel cell. From the evolution of the battery SOC, it can be

Table 7: Fuzzy rule base.

P_{dem}/SOC$_{bat}$	L	M	H
NB	S	S	S
NS	S	S	S
M	B	M	M
PS	TB	B	M
PB	TB	B	B

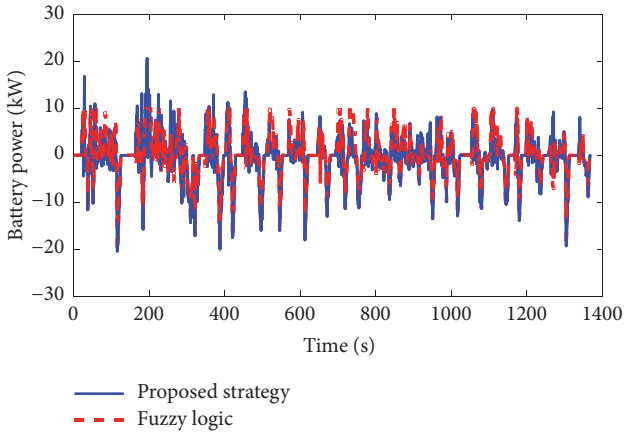

Figure 16: Comparison of the battery power between the proposed strategy and the fuzzy logic strategy.

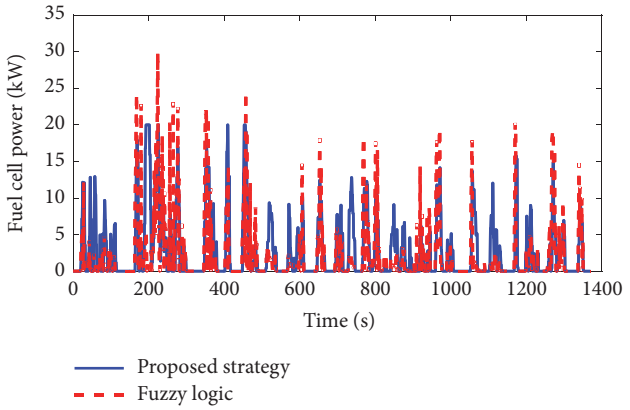

Figure 17: Comparison of the fuel cell power between the proposed strategy and the fuzzy logic strategy.

obviously found that the SOC fluctuates more frequently to participate in the power distribution over the whole driving cycle by the proposed strategy. Besides, the SOC is also regulated within a reasonable fluctuation range for ensuring the battery has enough space for absorbing the peak or regenerative power.

5. Conclusion

In this paper, a game theory energy management strategy for a fuel cell/battery hybrid energy storage system has been proposed. The competing interaction between the fuel cell and the battery has formulated a noncooperative game,

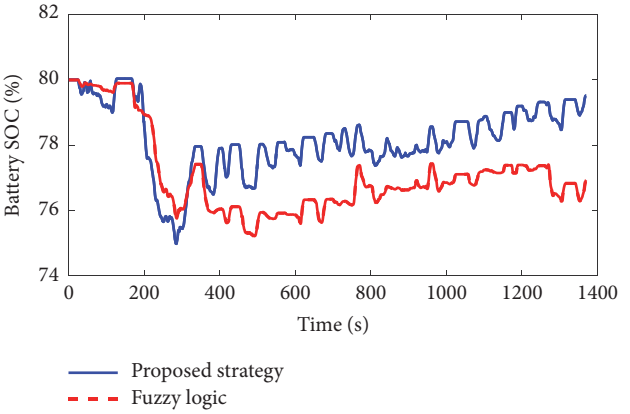

Figure 18: Comparison of the battery SOC between the proposed strategy and the fuzzy logic strategy.

in which each player pursues its own maximum utility depending on the power demand information. The uncertain behavior of the power demand due to inaccurate prediction of driving cycle has been considered when the utility function is designed for each player. Iterative algorithm has been designed to implement the strategy by introducing a fuzzy logic controller for correction. Comparison results reveal that the proposed method can effectively reduce the influence of the prediction accuracy on the Nash Equilibrium. Both the cost of the fuel economy and the battery degradation are concurrently curtailed to a minimum level.

This study tries to propose a new approach for solving energy management problem of a fuel cell/battery hybrid energy storage system. Its effectiveness has been fully demonstrated by comparison analysis. However, the proposed approach needs deep knowledge of the each control plant and therefore cannot be directly extrapolated to other hybridizations with different power sources. This constitutes one of the main disadvantages.

Data Availability

The Matlab data used to support the findings of this study are included within the article. The specific iteration process of the algorithm is also described in the paper.

Conflicts of Interest

The authors declare that they have no conflicts of interest.

Acknowledgments

This work is supported by Project of Liaoning Province Major Technology Platform, Grant JP2017002; Guidance Plan of Natural Science Foundation of Liaoning Province, Grant 20180551280; National Science Foundation of China, Grant 51675257; Project of Liaoning Province Innovative Talents, Grant LR2016054.

References

[1] S. F. Tie and C. W. Tan, "A review of energy sources and energy management system in electric vehicle," *Renewable & Sustainable Energy Reviews*, vol. 20, pp. 82–102, 2013.

[2] T. Matsumoto, N. Watanabe, H. Sugiura, and T. Ishikawa, "Development of Fuel-Cell Hybrid Vehicle," in *Proceedings of the SAE 2002 World Congress & Exhibition*, pp. 4–7, Detroit, Mich, USA, March 2002.

[3] J. Larminie and A. Dicks, *Fuel Cell Systems Explained*, Wiley, West Sussex, UK, 2000.

[4] G. Ren, G. Ma, and N. Cong, "Review of electrical energy storage system for vehicular applications," *Renewable & Sustainable Energy Reviews*, vol. 41, pp. 225–236, 2015.

[5] W. Gao, "Performance comparison of a fuel cell-battery hybrid powertrain and a fuel cell-ultracapacitor hybrid powertrain," *IEEE Transactions on Vehicular Technology*, vol. 54, no. 3, pp. 846–855, 2005.

[6] J. Bauman and M. Kazerani, "A comparative study of fuel-cell-battery, fuel-cell-ultracapacitor, and fuel-cell-battery-ultracapacitor vehicles," *IEEE Transactions on Vehicular Technology*, vol. 57, no. 2, pp. 760–769, 2008.

[7] P. Garcia, L. M. Fernandez, C. A. Garcia, and F. Jurado, "Energy management system of fuel-cell-battery hybrid tramway," *IEEE Transactions on Industrial Electronics*, vol. 57, no. 12, pp. 4013–4023, 2010.

[8] S. Kelouwani, K. Agbossou, Y. Dubé, and L. Boulon, "Fuel cell plug-in hybrid electric vehicle anticipatory and real-time blended-mode energy management for battery life preservation," *Journal of Power Sources*, vol. 221, pp. 406–418, 2013.

[9] H. Hemi, J. Ghouili, and A. Cheriti, "A real time fuzzy logic power management strategy for a fuel cell vehicle," *Energy Conversion and Management*, vol. 80, pp. 63–70, 2014.

[10] Q. Li, W. Chen, Y. Li, S. Liu, and J. Huang, "Energy management strategy for fuel cell/battery/ultracapacitor hybrid vehicle based on fuzzy logic," *International Journal of Electrical Power & Energy Systems*, vol. 43, no. 1, pp. 514–525, 2012.

[11] J. P. Ribau, C. M. Silva, and J. M. C. Sousa, "Efficiency, cost and life cycle CO2 optimization of fuel cell hybrid and plug-in hybrid urban buses," *Applied Energy*, vol. 129, pp. 320–335, 2014.

[12] O. Hegazy and J. Van Mierlo, "Optimal power management and powertrain components sizing of fuel cell/battery hybrid electric vehicles based on particle swarm optimisation," *International Journal of Vehicle Design*, vol. 58, no. 2-4, pp. 200–222, 2012.

[13] J. P. Trovão, P. G. Pereirinha, H. M. Jorge, and C. H. Antunes, "A multi-level energy management system for multi-source electric vehicles—an integrated rule-based meta-heuristic approach," *Applied Energy*, vol. 105, pp. 304–318, 2013.

[14] C.-Y. Li and G.-P. Liu, "Optimal fuzzy power control and management of fuel cell/battery hybrid vehicles," *Journal of Power Sources*, vol. 192, no. 2, pp. 525–533, 2009.

[15] L. Xu, M. Ouyang, J. Li, and F. Yang, "Dynamic Programming Algorithm for minimizing operating cost of a PEM fuel cell vehicle," in *Proceedings of the 2012 IEEE 21st International Symposium on Industrial Electronics (ISIE)*, pp. 1490–1495, Hangzhou, China, May 2012.

[16] S. Maharjan, Q. Zhu, Y. Zhang, S. Gjessing, and T. Başşar, "Dependable demand response management in the smart grid: A stackelberg game approach," *IEEE Transactions on Smart Grid*, vol. 4, no. 1, pp. 120–132, 2013.

[17] B. Chai, J. Chen, Z. Yang, and Y. Zhang, "Demand response management with multiple utility companies: A two-level game approach," *IEEE Transactions on Smart Grid*, vol. 5, no. 2, pp. 722–731, 2014.

[18] K. Wang, Z. Ouyang, R. Krishnan, L. Shu, and L. He, "A game theory-based energy management system using price elasticity for smart grids," *IEEE Transactions on Industrial Informatics*, vol. 11, no. 6, pp. 1607–1616, 2015.

[19] S. Mei, Y. Wang, F. Liu, X. Zhang, and Z. Sun, "Game approaches for hybrid power system planning," *IEEE Transactions on Sustainable Energy*, vol. 2, no. 2, 2012.

[20] C. Dextreit and I. V. Kolmanovsky, "Game theory controller for hybrid electric vehicles," *IEEE Transactions on Control Systems Technology*, vol. 22, no. 2, pp. 653–663, 2014.

[21] M. Gielniak and Z. Shen, "Power management strategy based on game theory for fuel cell hybrid electric vehicles," in *Proceedings of the IEEE 60th Vehicular Technology Conference, 2004. VTC2004-Fall. 2004*, pp. 4422–4426, Los Angeles, CA, USA.

[22] H. Yin, C. Zhao, M. Li, C. Ma, and M.-Y. Chow, "A Game Theory Approach to Energy Management of An Engine-Generator/Battery/Ultracapacitor Hybrid Energy System," *IEEE Transactions on Industrial Electronics*, vol. 63, no. 7, pp. 4266–4277, 2016.

[23] Q. Zhang, W. Deng, and G. Li, "Stochastic Control of Predictive Power Management for Battery/Supercapacitor Hybrid Energy Storage Systems of Electric Vehicles," *IEEE Transactions on Industrial Informatics*, vol. 14, no. 7, pp. 3023–3030, 2018.

[24] Z. Chen, L. Li, B. Yan, C. Yang, C. Marina Martinez, and D. Cao, "Multimode Energy Management for Plug-In Hybrid Electric Buses Based on Driving Cycles Prediction," *IEEE Transactions on Intelligent Transportation Systems*, vol. 17, no. 10, pp. 2811–2821, 2016.

[25] H. Hemi, J. Ghouili, and A. Cheriti, "Combination of Markov chain and optimal control solved by Pontryagin's minimum principle for a fuel cell/supercapacitor vehicle," *Energy Conversion and Management*, vol. 91, pp. 387–393, 2015.

[26] B. Asadi and A. Vahidi, "Predictive Cruise Control: Utilizing Upcoming Traffic Signal Information for Improving Fuel Economy and Reducing Trip Time," *IEEE Transactions on Control Systems Technology*, vol. 10, no. 17, pp. 2811–2821, 2016.

[27] C. Zhang, A. Vahidi, P. Pisu, X. Li, and K. Tennant, "Role of terrain preview in energy management of hybrid electric vehicles," *IEEE Transactions on Vehicular Technology*, vol. 59, no. 3, pp. 1139–1147, 2010.

[28] X. Hu, J. Jiang, B. Egardt, and D. Cao, "Advanced power-source integration in hybrid electric vehicles: multicriteria optimization approach," *IEEE Transactions on Industrial Electronics*, vol. 62, no. 12, pp. 7847–7858, 2015.

[29] J. Wang, P. Liu, J. Hicks-Garner et al., "Cycle-life model for graphite-LiFePO$_4$ cells," *Journal of Power Sources*, vol. 196, no. 8, pp. 3942–3948, 2011.

[30] Z. Song, H. Hofmann, J. Li, X. Han, X. Zhang, and M. Ouyang, "A comparison study of different semi-active hybrid energy storage system topologies for electric vehicles," *Journal of Power Sources*, vol. 274, pp. 400–411, 2015.

[31] M. A. Abido, "Optimal power flow using particle swarm optimization," *International Journal of Electrical Power & Energy Systems*, vol. 24, no. 7, pp. 563–571, 2002.

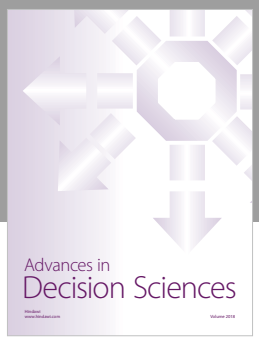

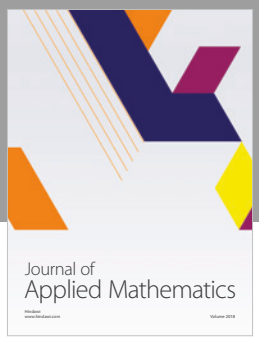

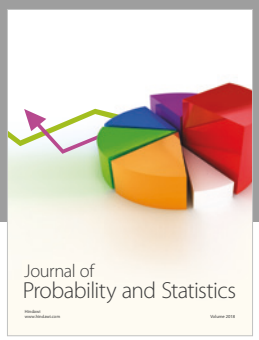

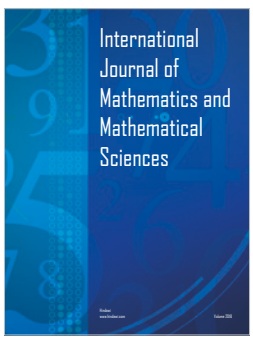

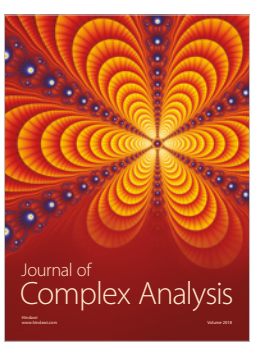

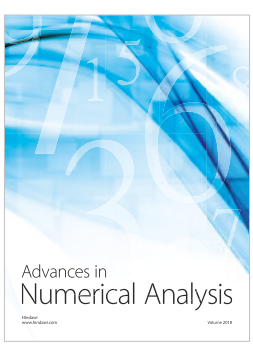

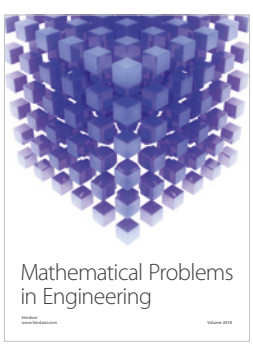

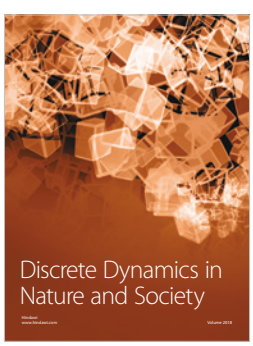

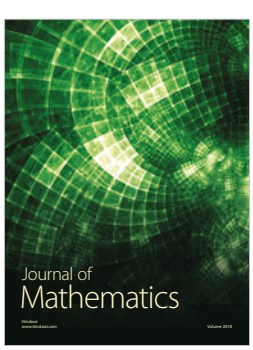

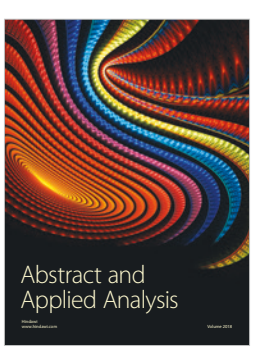

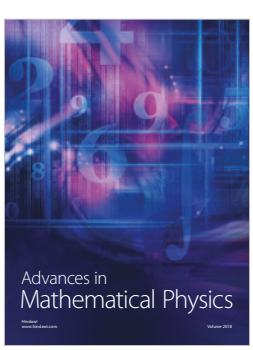

Hindawi

Submit your manuscripts at
www.hindawi.com